ACS OMEGA

http://pubs.acs.org/journal/acsodf

Article

Evaluating CO_2 Capture Performance of Trisolvent MEA–BEA–AMP with Heterogeneous Catalysts in a Novel Bench-Scale Pilot Plant

Nan Zhang, Huancong Shi,* Hanyun Wang, Yongcheng Feng, Jing Jin,* Paitoon Tontiwachwuthikul,* and Mengxiang Fang*

Cite This: ACS Omega 2024, 9, 1838–1849

Read Online

ACCESS | Metrics & More | Article Recommendations | Supporting Information

ABSTRACT: To reduce the huge energy cost of CO_2 capture technology applicable in industry, the CO_2 absorption–desorption performance was conducted in a novel bench-scale pilot plant with hot water as a heat source. The trisolvent MEA(monoethanol amine)–BEA(butylethanol amine)–AMP(2-amino-2-methyl-1-propanol) was prepared at a specific concentration to analyze the CO_2 capture performance and compared with 5 M MEA as the benchmark. Meanwhile, several solid acid catalysts, blended H-ZSM-5/γ-Al_2O_3(1/2), or HND-8, were packed in the desorber, and the solid base catalyst, $CaCO_3$ or $CaMg(CO_3)_2$, was packed in the absorber with random packing. The CO_2 absorption efficiency (AE), cyclic capacity (CC), and heat duty (HD) were tested onto MEA–BEA–AMP and MEA under various operating conditions. Experimental results indicated that the performance of 4.3 mol/L MEA–BEA–AMP was significantly better than 5 M MEA under both catalytic and noncatalytic operation. The most energy efficient combination of this study was discovered as 0.3 + 2 + 2 mol/L MEA–BEA–AMP, with 50 g ($CaCO_3$/$CaMg(CO_3)_2$) in the absorber and 150 g H-ZSM-5/γ-Al_2O_3(1/2) in the desorber. The heat duty reached as low as 2.4 GJ/tCO_2 at a F_G of 7.0 L/min and a F_L of 70 mL/min. These results were highly applicable in an industrial amine scrubbing pilot plant for CO_2 capture.

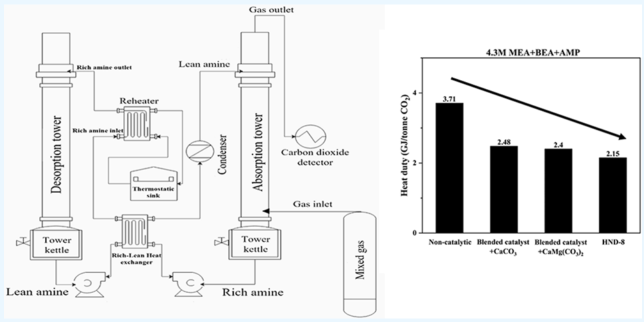

1. INTRODUCTION

Effective CO_2 capture, utilization, and storage (CCUS) technology was one of the most important technologies in coal-fired power industry to achieve the goals of net-zero CO_2 emission. Postcombustion carbon capture (PCCC) using amine-based solvents turns out to be the most suitable technology for flue gas decarbonization based on massive gas flux and low CO_2 concentration.[1,2] The chemisorption in an amine scrubbing process in a pilot plant was possibly the most effective way to suit large-scale CO_2 reduction and capture.[3,4] However, the huge energy cost of CO_2 desorption in carbon capture accounts for 70% of the total cost, which is the main challenge faced by PCCC technology.[5−7] High operating temperatures (120–140 °C) with steam as a heat source were the main reason for the side effects such as high energy costs, solvent loss and amine degradation, stress cracking corrosion, etc.[8]

Previously, intensive fundamental studies have been conducted into the heat duty reduction, and these reviews had reached an agreement;[8−12] there were three energy efficient solutions which were solvent improvement,[13,14] process intensification,[13,15] and heterogeneous catalysis.[16,17] After 2016, several research studies were focused on the research of steady-state process, which was more realistic toward industrial application.[18−21] These studies were focused on the steady-state operation process and adopted the verified good performance amine solvents and catalysts from publications directly, in order to evaluate their performance in a bench-scale pilot plant to mimic industrial application.

Alivand et al. published a review of more than 40 types of solid acid catalysts for heat duty reduction[16] and reported that these catalysts were able to work on MEA solvents to desorb CO_2 below 100 °C, the boiling point of the water. This review also reported another novel process to run solid catalysts,[16] which is the "catalyst-packed bench-scale CO_2 absorption process with an extra heat exchanger and hot water as the heat source." Low desorption temperatures below 100 °C could effectively reduce corrosion and solvent degradation and mitigate the other side effects of CO_2 absorption processes.[22] This technology aims to replace high-pressure steam with hot water as a reliable source of energy for catalytic postcombustion CO_2 capture.

Since 2017, Idem's group reported several studies based on the combination of "blended amine" + "solid acid or base

Received: October 27, 2023
Revised: December 4, 2023
Accepted: December 11, 2023
Published: December 25, 2023

catalysts" + "catalyst-packed bench-scale process."[23−27] These publications reported the MEA,[23] MEA−MDEA,[24,28] and BEA−AMP biblend solvents,[26,27,29] with solid acid catalysts as γ-Al_2O_3[23,24] or H-ZSM-5[23−25] and solid base as $BaCO_3$,[26] $CaCO_3$,[26] or K/MgO.[25,26] These results reported very good cyclic capacity and relatively low heat duty, which is meaningful. These studies focused on the effect of solid acid catalysts γ-Al_2O_3[23,24] or H-ZSM-5 on AE, CC, and HD in discussion.[23−27]

Besides solid acid catalysts, the solid base was adopted to accelerate CO_2 absorption, and based on kinetics,[30] electrons are needed to promote the CO_2 absorption rate. Therefore, $CaCO_3$,[31−34] $MgCO_3$,[34−36] and $CaMg(CO_3)_2$ were selected as Lewis base catalysts, which were good electron donors.

For the blended amine for the process, an amine selection chart was published in 2017,[37] which discovered two good performance single amines, BEA and AMP, with superior absorption−desorption parameters.[37] Later on, Shi et al. studied the MEA−BEA−AMP[38−40] at a specific ratio of 0.3/2/2 to fully use the coordinative effect[41−43] (details are given in the Supporting Information). When compared with 4.0 M BEA−AMP, the 4.3 M MEA−BEA−AMP trisolvent exhibited better absorption and desorption performance by 10−30%.[38−40] Therefore, the trisolvent MEA−BEA−AMP at a specific ratio (0.3/2/2 mol/L) was selected particularly for this study based on its absorption−desorption parameters with the aid of both solid base and acid catalysts.[39]

Finally, this study introduced a catalyst-aided bench-scale process, with the combination of 0.3 + 2 + 2 mol/L MEA−BEA−AMP, with solid acid (blended γ-Al_2O_3/H-ZSM-5 = 2:1, and HND-8) and solid base ($CaCO_3$ and $CaMg(CO_3)_2$) to evaluate its operation under steady state. The blended ratio of γ-Al_2O_3/H-ZSM-5 was adopted from a previous study.[33] The experimental device was similar to Idem's previous work,[23,24] but our device was bigger. The amine was trisolvent instead of bisolvent (4.3 M MEA−BEA−AMP vs 4 M BEA−AMP). Although both solvents looked similar to each other, the absorption−desorption performance of trisolvent is better than bisolvent simultaneously, and this is the first time that trisolvent was studied on the bench-scale process. Although intensive studies reported and reviewed massive lab-scale synthesized solid acid/base catalysts,[16,17] the author's group focused on commercially available solid catalysts to ensure their stability and amount of products to fit the realistic implementations in industry.

The aim and purpose of this research is to (1) investigate the CO_2 absorption−desorption performance of 4.3 mol/L MEA−BEA−AMP with a combination of solid/base acid catalysts in a pilot plant to evaluate the effect of catalysts in the absorber and desorber. (2) The CO_2 absorption efficiency (AE), cyclic capacity (CC), and heat duty (HD) were conducted on the system to find out better operating conditions to achieve higher CC and low HD at AE > 90%.

2. THEORY

2.1. Calculations of Absorption Efficiency, Cyclic Capacity, and Heat Duty. Under steady state, the following variables were tested: inlet/outlet gas flow rate (F_G), liquid flow rate (F_L), temperate profile of the absorber and desorber (T), CO_2 concentration of inlet/outlet gas (X_{in} and X_{out}), and CO_2-loading of rich/lean amine $\alpha_{rich}/\alpha_{lean}$. These variables were detected, recorded, and used to calculate absorption efficiency, cyclic capacity, and heat duty according to eqs 1−5).[23−27]

$$\text{Absorption efficiency (AE)} = \frac{F_{G_1} \times X_{in} - F_{G_2} \times X_{out}}{F_{G_1} \times X_{in}} \tag{1}$$

where F_{G_1} and F_{G_2} are the volumetric flow rate of feed and off gas, respectively, and X_{in} and X_{out} are the CO_2 concentrations in the inlet and outlet gas, respectively. The absorption efficiency ought to be >90% to meet the CO_2 emission requirements.[23,24,26]

$$\text{Cyclic capacity (CC)} = F_L \times (\alpha_{rich} - \alpha_{lean}) \times C_A \tag{2}$$

where α_{rich} and α_{lean} are the rich and lean CO_2 loading, respectively. F_L is the volumetric flow rate of the solvent. C_A is the amine concentration. The cyclic capacity represented the CO_2 take up at standard time period. Some studies reported cyclic capacity as $(\alpha_{rich} - \alpha_{lean}) * C_A$ at constant F_L.[25,27] However, eq2 was used in this study due to different F_L.

$$\text{heat duty (HD) HD1} = \frac{m_{HM} \times C_{pHM} \times (T_{HM,in} - T_{HM,out})}{\dot{m}CO_2} \tag{3}$$

$$\dot{m}CO_2 = MW_{CO_2}\frac{F_{G_1} \times X_{in} - F_{G_2} \times X_{out}}{V_{CO_2}} \tag{4}$$

$$HD2 = \frac{m_{HM} \times C_{pHM} \times (T_{HM,in} - T_{HM,out})}{F_L \times (\alpha_{rich} - \alpha_{lean}) \times C_A \times MW_{CO_2}} \tag{5}$$

HD1 was calculated from CO_2 removal in the gas line,[23,24,26,27] and the $\dot{m}CO_2$ is the mass of CO_2 removal in the gas line. HD2 was calculated from CO_2 already absorbed in the liquid phase by means of CC × MW_{CO_2}.[23,26,27] m_{HM} is the mass flow rate of hot medium, and C_{pHM} is its heat capacity.[24] This study used eq 5) to evaluate HD, although the minute CO_2 gas may go via other exits (thermos couple or joint/connections) in the process.

The correlations of AE, CC, and HD were mainly on F_L, smaller F_L results in bigger CC and higher HD, but the AE will be decreased. Therefore, there is an optimizedFF_L for this set of experiments.

2.2. The Main Reaction Scheme within CO_2-trisolvent and Carbamate Breakdown. The reactions within MEA−BEA−AMP solutions are listed in reactions (1−7).[26] MEA and BEA are primary/secondary amines (RR′NH) that react with CO_2 to form carbamate and protonated amines through the zwitterion mechanism in reactions (1−2).[44] The carbamate breakdown and hydrolysis reactions are listed in reactions (3−7).[23,45] As for AMP (RNH_2), the carbamate is unlikely to occur due to its steric hindrance from the bulky group adjacent to the amino group, and the main product was bicarbonate.[37]

Carbamate formation via the Zwitterion mechanism:

$$RR'NH + CO_2 \leftrightarrow RR'NH^+{-}COO^- \text{ (zwitterion)} \tag{Reaction 1}$$

$$RR'NH^+{-}COO^- \text{ (zwitterion)} + RR'NH \leftrightarrow RR'N{-}COO^- \text{ (carbamate)} + RR'NH_2^+ \tag{Reaction 2}$$

Bicarbonate formation by CO_2 in water:

$$CO_2 + H_2O \leftrightarrow H_3O^+ + HCO_3^- \tag{Reaction 3}$$

https://doi.org/10.1021/acsomega.3c08021
ACS Omega 2024, 9, 1838−1849

Bicarbonate formation by carbamate hydrolysis:

$$RR'NCOO^- + H_2O \leftrightarrow RR'NH + HCO_3^- \quad \text{(Reaction 4)}$$

Without solid acid catalysts, the CO_2 desorption process undergoes two main reactions which are carbamate breakdown and amine deprotonation.[46−48]

Carbamate breakdown:

Proton transfer: $RR'NCOO^- + H_3O^+$

$$\leftrightarrow RR'NH^+{-}COO^- \text{ (zwitterion)} + H_2O \quad \text{(Reaction 5)}$$

N−C bond breaking: $RR'NH^+{-}COO^-$ (zwitterion)

$$\leftrightarrow RR'NH + CO_2 \quad \text{(Reaction 6)}$$

Amine deprotonation: $RR'NH^+ + H_2O$

$$\leftrightarrow RR'NH + H_3O^+ \quad \text{(Reaction}$$

The carbamate breakdown depends on the thermal energy provided and the availability of protons. Protons were provided from amine deprotonation reaction 7. Once the protons released from RNH_3^+, H^+ reacts with the N atom of carbamate ($RNHCOO^-$) resulting in switching the hybridization of the N and C atoms from sp^2 to sp^3 and stretching the N−C bond to weaken the bond strength.[16,49] The N−C bond finally breaks, and the zwitterion splits into CO_2 and RNH_2. Reaction 7 is a strongly endothermic and requires outside energies to overcome the energy barrier due to the high alkalinity of amine solvents, implying that carbamate breakdown was difficult to taking place at a low temperature with in adequate heat.[47]

3. EXPERIMENTAL APPARATUS AND PROCESS

3.1. Chemicals, Catalysts, and Sample Analysis. The amines MEA (≥99%), BEA (≥98%), and AMP (≥99%) were purchased from Guoyao Ltd. The CO_2/N_2 (15%/85%) mixed gas was purchased from Qingkuan gas Ltd. The pelletized solid catalysts $CaCO_3$, $CaMg(CO_3)_2$, H-ZSM-5, γ-Al_2O_3, and HND-8 were purchased from Yinghe Zibo Catalyst Ltd. Methyl orange was an indicator and HCl (1.0 mol/L) was used as a standard for titration. The CO_2 loading tests of various amine samples were tested with a Chittick apparatus by the Association of Official Analytical Chemists (AOAC).[50] This method has an error of ±2.5% based on CO_2 loading tests of ±0.5 L of CO_2 release, which was accurate for this study.

3.2. THE BENCH-SCALE PILOT PLANT AND EXPERIMENTAL PROCEDURES OF CO_2 ABSORPTION AND DESORPTION

3.2.1. The Catalyst-Packed Pilot-Plant with Hot Water as Heat Source. Figure 1 plots the schematic diagram of the experimental apparatus. The apparatus consisted of two towers made of stainless steel with a height of 3.94 ft (1.2 m) and an internal diameter of 1.97 in. (0.05 m). It contains a saturator, a hot-water-amine heat exchanger, two amine storage tanks with 4 L capacity, two pumps, a rich-lean heat exchanger, a hot water-rich amine heat exchanger, and flow meters. The peristaltic pump with a measuring range of 300 rpm is used for circulating. The speed flow of liquid flow rate was adjusted at 70−90 mL/L manually with constant value. The gas source used in this experiment simulates the actual flue gas, i.e., 15% CO_2 and 85% N_2 without O_2, NO_x, or SO_x. The gas flow rate (F_G) was determined with a gas flue meter, and the CO_2 concentration

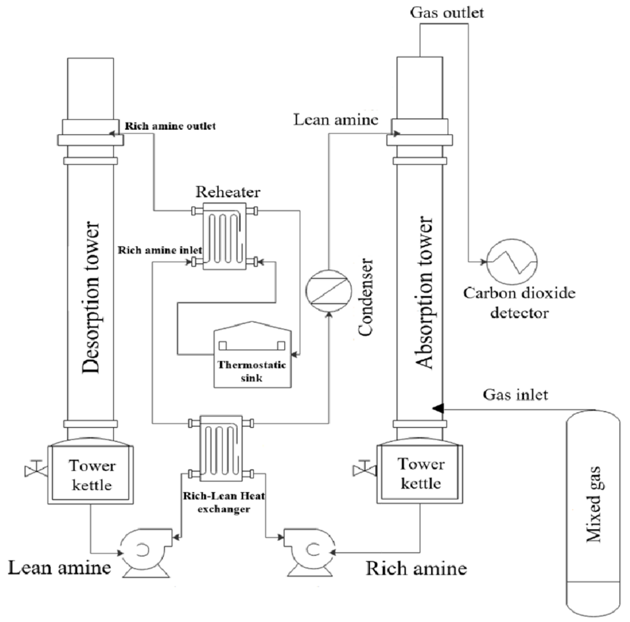

Figure 1. Schematic representation of the experimental apparatus for CO_2 capture.

(%) was analyzed with an analyzer. Six thermocouples are designed for the absorption/desorption towers to measure the temperature distribution with an interval of 0.20 m along different locations. Based on catalytic CO_2 desorption analysis, the desorber catalysts lose most of their strength at temperatures below 85 °C. The temperature profile in the desorber is an indicator to ensure the effect of solid catalysis although most of them were above 87−88 °C along the desorber. A K-type thermocouple was used with relatively stable performance and high accuracy for temperature measurement. The realistic photo of the pilot-plant iss listed in the Supporting Information.

The catalysts adopted random packing with inert marbles, as shown in Figure 2. The absorption tower adopted random packing with θ-type packing and inert marbles (0.008 and 0.006 m diameter). The base catalyst was blended with these marbled and packing materials. The layer of solid acid catalyst-packing

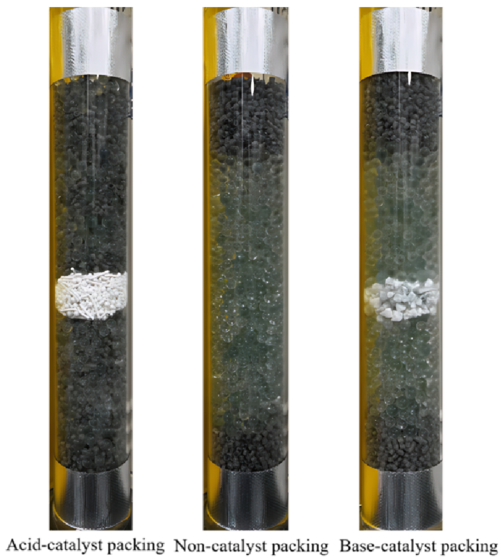

Figure 2. Photos of noncatalytic and catalytic packing for acid and base.

https://doi.org/10.1021/acsomega.3c08021
ACS Omega 2024, 9, 1838−1849

material was placed in the middle. The acid catalyst was mixed with small inert marbles (0.003 m) in the desorption tower. Larger marbles (0.008 m) were used on top and bottom sides to support the catalytic bed. Without catalysts, the layer was filled with inert small marbles (0.006 m). The amine solvents flew from the top of the tower to the bottom by gravity. The catalyst better be placed in the middle in order to analyze the effect accurately. The fresh catalysts were used for each test, and the amine solvents were circulated for 6−7 h for each run to reach steady state; there is little amine degradation based on the CO_2 loading, because the mixed gas has no O_2, NO_x, or SO_x inside. The stability of solid catalysts was guaranteed since they are commercial catalysts, and experiments were conducted with used catalysts which had little loss.

3.2.2. EXPERIMENTAL OPERATION PROCEDURE OF THE BENCH-SCALE PILOT-PLANT

The trisolvent was prepared in 4 L with α_{lean} at 0.20−0.25 mol/mol. The amine was pumped from the amine storage tank at a flow rate of 70 mL/min to the top of the absorber and went through the overall process including absorber, desorber, amine storage tank, lean-rich amine heat exchanger, and amine-hot water exchanger. Concurrently, the hot water bath was initiated and set at 95−98 °C to heat up the amine solvent in the hot water-rich solvent heat exchanger before it enters into the desorber. After amine solvent circulation was continuous with constant temperature , the mixed gas with 15% CO_2/85% N_2 was introduced to the absorption tower at the bottom via a gas flowmeter. The mixed gas reached the liquid lean amine flow in the absorber in a countercurrent way to start CO_2 absorption. The exit gas leaves the top of the absorber when 90−100% CO_2 is removed, and the rich amine solvent leaves the absorber at the bottom into the amine storage tank. The CO_2-rich amine solvent was heated first via a lean-rich amine exchanger and further heated to a temperature of 90 ± 2 °C via a hot water−amine heat exchanger and then to the top of the desorber. The CO_2 desorption was strengthened by the catalyst bed, and the CO_2-lean amine solvent leaves from the desorption tower and then cooled by rich amine and pumped into the absorption tower as a complete cycle. Each tower was installed with a condenser on the top to condense amine or water vapor exiting the tower. Therefore, the CO_2-absorption and desorption process reached the steady state, and the data can be recorded. It usually took about 6 h to reach steady state for the whole system. Table 1 summarizes the experimental operating conditions.

The CO_2 loadings and the amount of CO_2 in the treated gas were detected using a Chittick apparatus and an infrared (IR) gas analyzer, respectively.[26] The gas flow rates and liquid flow rates were tested with flowmeters, and the temperature profiles were detected with thermocouple. The monitor reported the digital data of F_G, F_L, T, and CO_2% in the gas phase as an integral.

Table 1. Operating Conditions in Bench-Scale Pilot Plant

condition	value
solvent used	5 M MEA, 4.3 M MEA−BEA−AMP
solvent flow rate	70, 80, 90 mL/min
feed gas flow rate	3.0 SLPM, 7.0 SLPM
CO_2 concentration in feed gas	15% CO_2 balance with 85% N_2
lean-amine inlet temperature	24−25 °C
absorber catalysts	$CaCO_3$, $CaMg(CO_3)_2$
rich-amine inlet temperature	88−90 °C
desorber catalysts	H-ZSM-5 (Si/Al = 19), γ-Al_2O_3, HND-8
weight of catalysts	100, 150, 200, 250 g
pressure in both towers	1 atm

4. RESULTS AND DISCUSSION

Results included four sections: (1) the effect of desorber catalysts on MEA as benchmark; (2) the effect of desorber catalysts on trisolvent MEA−BEA−AMP; (3) the effect of absorber−desorber catalysts on trisolvent; and (4) the CC and HD of trisolvent versus MEA to indicate its superior performance.

4.1. Effect of Desorber Catalysts on MEA Solvents.

4.1.1. Effect of Solid Acid on Absorption Efficiency. Figure 3 exhibits the effect of blended H-ZSM-5/γ-Al_2O_3 (2:1) on the absorption efficiency at F_G = 3.0 L/min and F_L of 70−90 mL/min. All the AEs under catalytic desorption were higher than noncatalytic tests (weight of catalysts W_{cat} = 0) in the y axis. The AE increased as the mass of H-ZSM-5/γ-Al_2O_3 (2:1) increased, and it reached a maximum of 100% at a W_{cat} hit 150 g. The AE was kept 100% until 250 g. At the same y axis, with increased F_L, the AE was increased under the same W_{cat}.

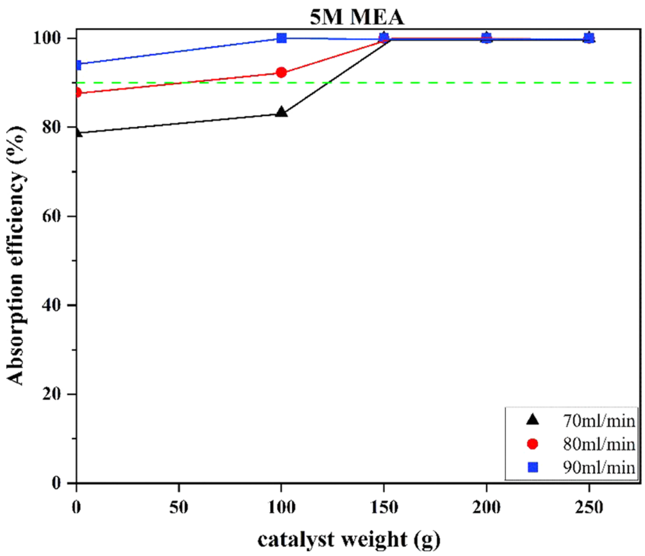

Figure 3. Effect of blended H-ZSM-5/γ-Al_2O_3 (2:1) catalysts on MEA with absorption efficiency at F_L = 70, 80, and 90 mL/min and fixed F_G = 3.0 L/min.

These results were similar to other studies, and the effect was verified with the MEA system repeatedly.[23,24] The intrinsic reason for Figure 3 was published:[24] the solid acid catalyst -packed desorber cannot only enhance the desorber performance but also indirectly increase the absorption efficiency.[25] As W_{cat} of H-ZSM-5/γ-Al_2O_3 (2:1) increases, the amine solvent with lower α_{lean} exit the desorber and pumped back to the absorber.[24] At 70 mL/min of 5.0 mol/L MEA circulation rate, the absorption capacity of lean amine decreased from 167.4 mmol CO_2/min to 158.85 mmol CO_2/min from noncatalyst to 150 g of H-ZSM-5/γ-Al_2O_3 (2:1). Less absorption capacity represented extra free MEA molecules in the MEA solvent to absorb CO_2, resulting in better AE.

4.1.2. Effect of Solid Acid Catalyst on Cyclic Capacity and Heat Duty. Figure 4a shows the cyclic capacity in the absence and presence of solid acid catalysts. The CC represents the

https://doi.org/10.1021/acsomega.3c08021
ACS Omega 2024, 9, 1838−1849

difference in CO_2 amount in rich and lean amine streams.[37] At constant F_L of 90 mL/min, the cyclic capacity increased from "noncatalytic" 16.80 mmol CO_2/min to "catalytic" 18.55−20.65 mmol CO_2/min with W_{cat} of 100−250 g H-ZSM-5/γ-Al_2O_3 (2:1). The catalytic system achieved higher CC than the noncatalytic system with 10.4%−22.9%.

The reason for the CC increase is the effect of solid acid catalysts, which facilitate carbamate breakdown via the zwitterion mechanism.[23] The detailed mechanism of catalytic carbamate breakdown with solid acid had been published repeatedly[16] (Supporting Information). This mechanism requires sufficient protons in the amine solvent. The proton was mainly released from $MEAH^+$ in the amine solution under noncatalytic condition. Deprotonation is a quite difficult step due to the strong basicity of MEA.[44]

AmineH$^+$ desorption

$$MEAH^+ + H_2O \leftrightarrow MEA + H_3O^+ \quad \text{(Reaction}$$

Carbamate breakdown

$$\begin{aligned} MEACOO^- + H_3O^+ \\ \leftrightarrow \text{zwitterion} \\ \leftrightarrow MEA + H_2O + CO_2 \end{aligned} \quad \text{(Reaction 9)}$$

However, when H-ZSM-5/γ-Al_2O_3 (2:1) was introduced, the proton donor facilitates the carbamate breakdown process. The carbamate ($MEACOO^-$) reacts with H^+ on the catalyst surface instead of $MEAH^+$ deprotonation reaction.[51] With an increased W_{cat} of H-ZSM-5/γ-Al_2O_3 (2:1), the amount of protons increased. Thus, CC increased with increased W_{cat}.[23,24]

Figure 4 reports the heat duty of 5.0 M MEA at 70−90 mL/min. Each curve represented the same F_L and F_G. From each curve, with an increased W_{cat}, the HD decreased to a minimum and increased slightly. These phenomena were reasonable, since the CC lies in the denominator of HD in eq 5.[24] The CC increased and reached a maximum in Figure 4a and decreased a little. The HD of F_L = 70 mL/min decreased from 12.67 GJ/tCO_2 to the minimum 11.14 GJ/tCO_2 and increased slightly to 11.32 GJ/tCO_2.

Furthermore, higher F_L represents higher HD for MEA solvent. This was reasonable, since HD can be calculated with eqs 3 and 4 from the gas line.[23] Since the AE of 5.0 M MEA almost reached 100% at various F_L, the $\dot{m}_{CO2}$ was constant as denominator. In eq 3, the numerator increased with increased F_L, and then the HD increased as consequence. With inadequate gas input in the process, the increase in F_L will not enhance CO_2 removal but raise the heat input and heat cost. Therefore, there is an optimized F_L/F_G in the system. Similar to other studies,[23,24] the absolute values of HD were above 10 GJ/tCO_2 for MEA system, too high in industry, so that a better amine solvent was required for the steady-state process.[26]

4.2. Effect of the Solid Acid Catalysts in Desorber on Trisolvents 4.3 M MEA−BEA−AMP.

The catalysis was focused on: (1) the effect on AE; (2) the effect on CC; (3) the effect on HD; (4) the temperature profiles in the absorber−desorber with catalysis.

4.2.1. Effect of Catalyst and Amine Flow Rate on Absorption Efficiency. The absorption efficiency (AE) is plotted in Figure 5, with a F_G of 7.0 L/min and a F_L of 70−90 mL/min, with a blended H-ZSM-5/γ-Al_2O_3 (2:1) catalyst used. From Figure 5, the trisolvents reached AE > 90%, and most cases reached 100%. Comparing to 3.0 L/min F_G at MEA, MEA−BEA−AMP exhibited superior absorption performance. For each curve with constant F_L, AE increased and reached the maximum of 100% with increased W_{cat} > 100 g. After 100 g, increased F_L cannot enhance AE anymore. Hence, the suitable F_L was 70 mL/min with a F_G of 7.0 L/min of this trisolvent for pilot plant for this study.

The intrinsic reason was the same as that in Section 4.1.1 for MEA solvent: the increased W_{cat} decreased α_{lean} of amine, releasing more free amine molecules to enhance CO_2 absorption. For noncatalytic absorption (W_{cat} = 0), the higher F_L resulted in higher absorption based on several phenomena: (1) increased liquid circulation leads to the increase in the surface area of wet packing and increased mass transfer.[52] (2) Higher F_L resulted in higher liquid mass transfer coefficient K_{Lav}, which directly increases the overall mass transfer coefficient K_{Gav}.[53]

4.2.2. Effect of Solid Acid Catalyst on Cyclic Capacity. The cyclic capacity was an important parameter for pilot plant, which represents the CO_2 take up for each cycle.[27] Figure 6 plotted the

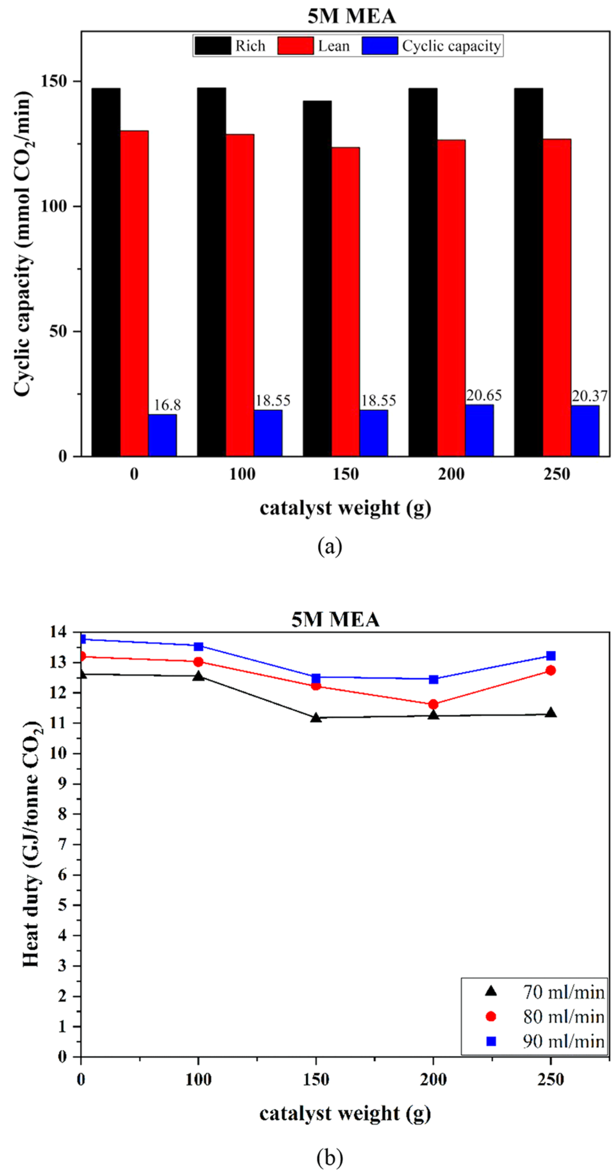

Figure 4. Effect of the solid acid catalyst on (a) cyclic capacity and (b) heat duty of MEA at F_L of 70, 80, and 90 mL/min and fixed F_G = 3.0 L/min.

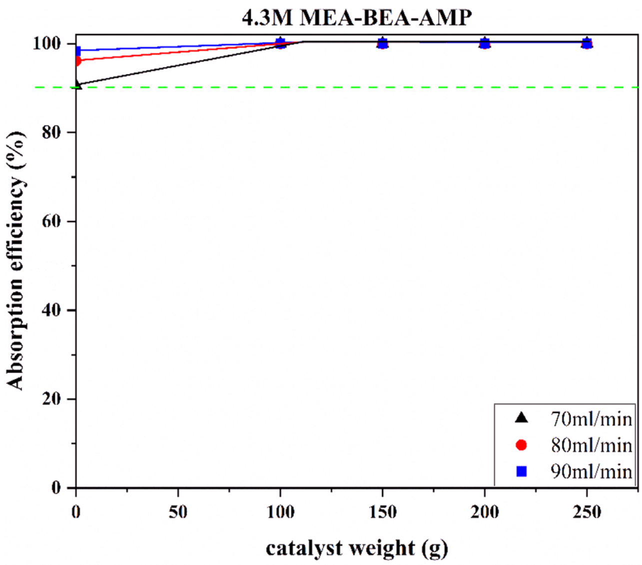

Figure 5. Effect of solid acid catalysts on absorption efficiency of MEA−BEA−AMP at F_L of 70, 80, and 90 mL/min.

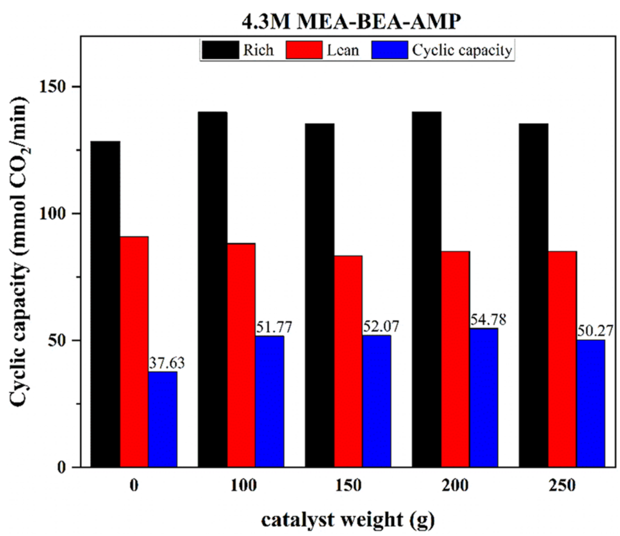

Figure 6. Effect of blended catalyst H-ZSM-5/γ-Al_2O_3 (2:1) on cyclic capacity of MEA−BEA−AMP at a F_L of 70 mL/min.

catalytic effect of CC with W_{cat} = 0−250 g H-ZSM-5/γ-Al_2O_3 (2:1), indicating the CC increased from 37.63 mmol CO_2/min in the noncatalytic to 50.27−54.78 mmol CO_2/min with catalysts. For catalytic tests, the CC reached the maximum at 200 g of catalysts.

The reason for the enhancement of solid catalysts H-ZSM-5 and γ-Al_2O_3 was clear:[23,24] the proton donor (Brønsted acid) catalysts enhanced the CO_2 desorption rate by means of extra H^+ available on the surface. The carbamate (RR′NCOO$^-$) of MEA and BEA reacts with existing protons on the catalyst instead of waiting for the amine deprotonation step to occur.[25−27,51] Then the absorption capacity of lean amine (red bar graph) decreased along with an increased W_{cat}.

Figure 7 plots the cyclic capacity without and with 150 g of solid acid catalysts: H-ZSM-5/γ-Al_2O_3 (2:1) and HND-8. The CC increased from 37.63 mmol CO_2/min W_{cat} = 0−52.07 mmol/CO_2/min for H-ZSM-5/γ-Al_2O_3 (2:1) and 61.19 mmol CO_2/min with HND-8. Both acid catalysts contain Brønsted

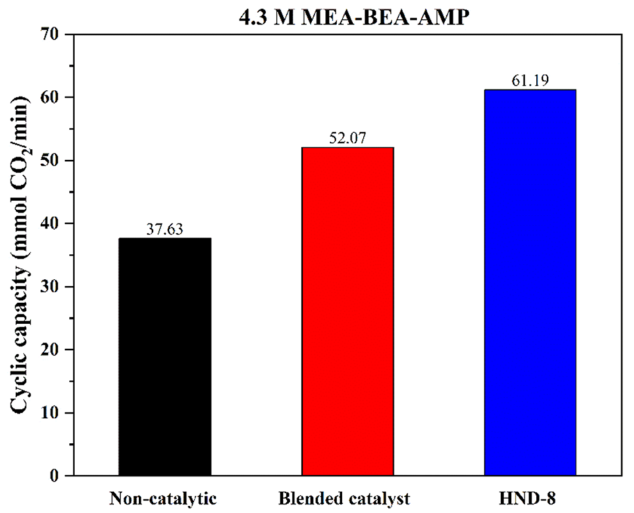

Figure 7. Effect of solid acid catalysts (150 g) on cyclic capacity of MEA−BEA−AMP at a F_L of 70 mL/min.

acid sites, which provide protons to attack carbamate (RNHCOO$^-$) directly to release amine and CO_2.[54,55]

The cyclic capacity ranked as follows: HND-8 > H-ZSM-5/γ-Al_2O_3 (2:1) > noncatalyst, reflecting the acidic strength of catalysts. The characteristics of both catalysts were categorized in Table 2, and the average pore size and acidic strength of γ-Al_2O_3, H-ZSM-5, and H-mordenite were published repeatedly in a recent review.[16] The HND-8 catalyst exhibits much higher acid strength than H-ZSM-5 and the γ-Al_2O_3 catalyst. Its larger pore size resulted in better CO_2 desorption performance and the faster reaction kinetics.[56,57] From Table 2, the HND-8 catalyst possessed a larger pore size than H-ZSM-5 and γ-Al_2O_3. The carbamate ion is a large molecule; so that smaller pore size limited its diffusion access while larger pore size facilitated the diffusion of carbamate species to reach the active sites onto the catalyst surface. Consequently, carbamate breakdown was easier to occur with HND-8 than with others, resulting in a high CO_2 desorption rate to higher cyclic capacity.

Table 2. Properties of Solid Acid Catalysts

catalyst	BET surface area (m^2/g)	average pore size	acid strength
H-ZSM-5 (Si/Al = 19)	290	2.2	0.4172
γ-Al_2O_3	381.9486	4.55	0.4830
HND-8	>20	**≥15**	**24.75**

4.2.3. Effect of Solid Acid Catalyst on Heat Duty. The effect on heat duty is plotted in Figure 8. Each curve represents F_L of 70, 80, and 90 mL/min with W_{cat} = 0−250 g H-ZSM-5/γ-Al_2O_3 (2:1). Higher F_L represents higher HD, the same reason as MEA in Section 4.1.2: since the AE reached 100%, the $\dot{m}CO_2$ was constant as denominator in eq 4. From eq 3 of HD calculation, higher F_L requires higher heat input. The trend of three curves was similar to each other, so that the lowest curve was discussed in detail.

In an experimental aspect, a lower F_L resulted in a lower heat duty based on two reasons: (1) smaller F_L resulted in bigger α_{rich} of amine solution entering the desorber. At a 70 mL/min circulation rate without catalysts, α_{rich} is around 0.5375 mol of CO_2/mol, while α_{rich} is 0.4687 and 0.4472 mol of CO_2/mol at 80 and 90 mL/min. A higher α_{rich} favored the desorption process.[25]

https://doi.org/10.1021/acsomega.3c08021
ACS Omega 2024, 9, 1838−1849

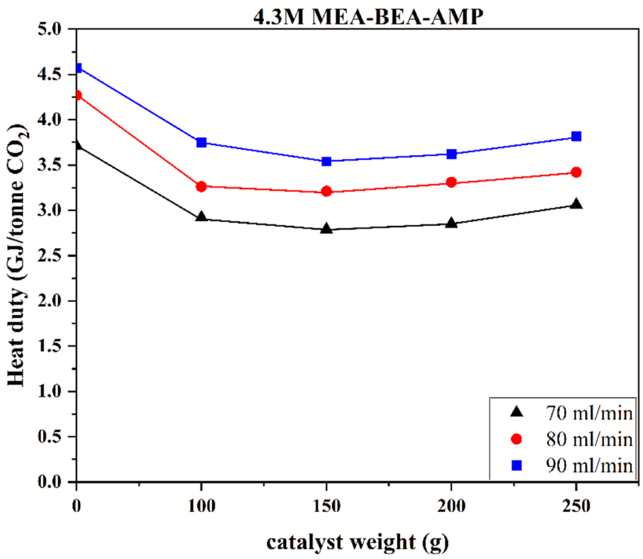

Figure 8. Effect of blended catalyst H-ZSM-5/γ-Al_2O_3 (2:1) on heat duty of MEA−BEA−AMP at F_L= 70, 80, 90 mL/min.

(2) Smaller F_L resulted in higher ratio of W_{cat}/ F_L, representing more amount of catalysts onto each mol of amine. The HD decrease at the lower F_L with fixed W_{cat}.[23]

At F_L of 70 mL/min, the HD decreased down to 2.79 GJ/tCO_2 at 150 g W_{cat}, and then increased a little at 200−250 g. With extra amount of W_{cat} such as 200 and 250 g, the CC of Figure 6 starts to decrease a little because α_{rich} was decreased while α_{lean} was almost the same. From eq 5, at the same F_L, the HD was mainly determined by (α_{rich}−α_{lean}) ∗ C_A.[24] Extra W_{cat} reduced not only α_{lean} but also α_{rich} as a side effect. Therefore, the optimized W_{cat} of the trisolvent was 150 g.

Finally, the HD is plotted in Figure 9 at 150 g W_{cat} as optimum. Based on Figure 9, the HD of noncatalytic tests was 3.71 GJ/tCO_2. The HD with H-ZSM-5/γ-Al_2O_3 (2:1) was reduced to 2.79 GJ/tCO_2, and the HD with HND-8 reached the minimum of 2.15 GJ/tCO_2. The HD was reduced to 24.8% and 42.1% with catalysts. The advantage of HND-8 was verified again.

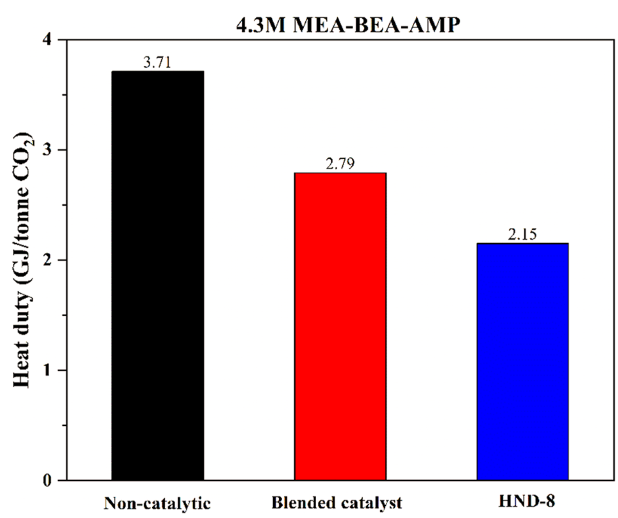

Figure 9. Effect of solid acid catalysts on heat duty of trisolvents at a F_L of 70 mL/min.

4.2.4. Effect of Desorber Catalyst on Temperature Profiles. Generally, the temperature was detected as 25−27 °C at the inlet input of amine solvent, while it increased to 35−40 °C along the absorption tower based on reaction heat release. For the desorber, the *T* was detected at 90−92 °C in the inlet, and it starts to cool down to 85−88 °C with CO_2 desorption reaction taking place. Along the desorber, the temperature is higher at 83−85 °C for lean liquid exiting the bottom of desorption tower, the intra heat exchanger of hot/cold liquids decreases the temperature first, and an additional cooling device is adopted to cool the amine solvent at a constant temperature of 25 °C, which flew back to the absorber.

The temperature profiles along the absorber are plotted in Figure 10a with/without acid catalysts. The temperature profile reflected the heat generation of CO_2 absorption reactions based on the exothermic reaction.[19] There was a temperature bulge at the bottom of the absorber since massive heat was released out of the CO_2 absorption. Higher reaction rates resulted in greater heat release and the wider temperature bulge along the absorber.[25] The highest temperature reached approximately 34 °C for the noncatalytic system, while it reached approximately 42 and 44 °C for H-ZSM-5/γ-Al_2O_3 (2:1) and HND-8 catalysts. The higher temperature bulge with catalysts was because of wider CO_2 loading range of amine solvents, which is 0.302−0.427 mol/mol (noncatalyst), 0.277−0.450 mol/mol (blended), and 0.303−0.506 mol/mol (HND-8). A wider CO_2 loading range indicated that more CO_2 was reacted in the absorber with more heat release.

The temperature profiles of the desorber are plotted in Figure 10b for catalytic and noncatalytic tests. The amine solution entered the top of desorber at 90.5−91.5 °C, and then started to decrease down to 85.5−86.5 °C. This decrease was reasonable since CO_2 desorption is strong endothermic reaction, the heat input was used into carbamate breakdown and CO_2 emission.[25] The order of the line was HND-8 > blended > noncatalyst, and the higher temperature represents better desorption performance.

4.3. Effect of Absorber−Desorber Catalyst on Trisolvents MEA−BEA−AMP. The 150 g acid catalyst H-ZSM-5/γ-Al_2O_3 (2:1) was packed in the desorber, and two base catalysts 150 g ($CaCO_3$/$CaMg(CO_3)_2$) were packed in the absorber to investigate the coordinative effect of acid−base catalysts. The calcium carbonate and dolomite ($CaCO_3$/$CaMg(CO_3)_2$) can significantly enhance the absorption rates compared with noncatalytic counterparts based on the author's study (Supporting Information). We fixed the W_{cat} of solid base for this study, and the effect of W_{cat} versus absorption await future study.

4.3.1. Effect of Both Catalysts on Absorption Efficiency. Figure 11 plots the absorption efficiency of both catalysts. The AE increased from 90.5% in the noncatalytic process to 100% catalytic process. The AE of the good performance trisolvent already reached 100% as optimum with solid acid, extra solid base cannot increase AE any more. Based on the literature study, the solid base did accelerate the CO_2 absorption process in many cases.[17]

4.3.2. Effect of Catalysts on Cyclic Capacity. Table 3 lists the α_{lean} and α_{rich} of trisolvents from different acid−base catalysts given in Figure 11. With the aid of a solid acid catalyst, the α_{lean} decreased from 0.302 to 0.277 mol/mol because of the catalysis on carbamate breakdown. The α_{rich} increased from 0.427 to 0.45 mol/mol based on leaner amine solvents. Furthermore, with the aid of solid base, both α_{lean} and α_{rich} increased properly, the α_{rich}

https://doi.org/10.1021/acsomega.3c08021
ACS Omega 2024, 9, 1838−1849

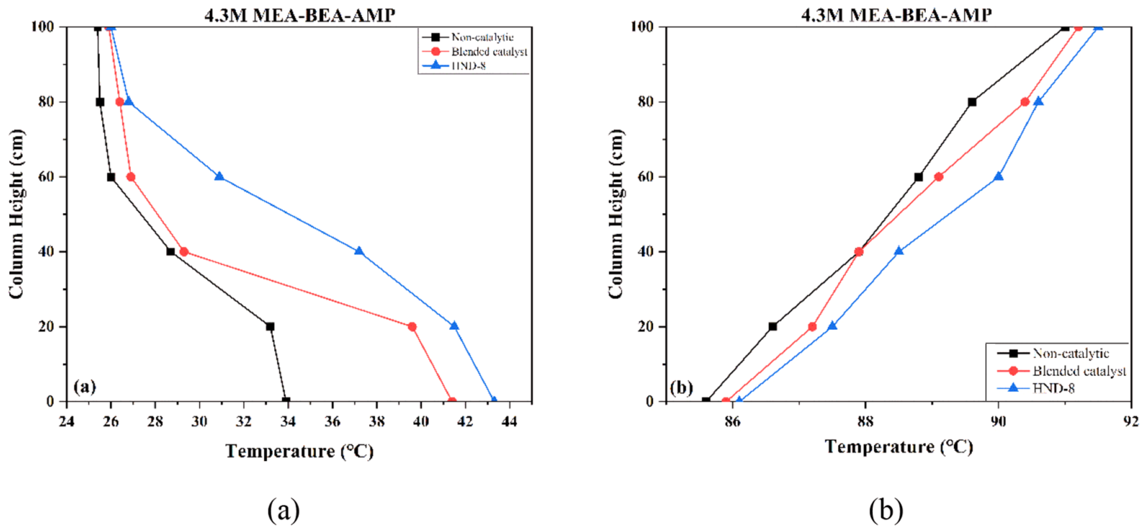

Figure 10. Effect of the solid acid catalyst on temperature profiles of the MEA−BEA−AMP in the (a) absorption and (b) desorption process.

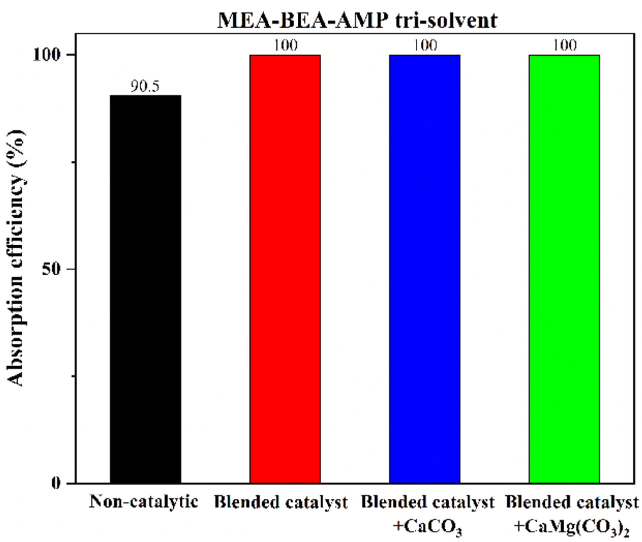

Figure 11. Effect of acid−base catalysts (H-ZSM-5/γ-Al_2O_3 (2:1)-$CaCO_3$/$CaMg(CO_3)_2$) (150 g + 150 g) on absorption efficiency at a F_L of 70 mL/min.

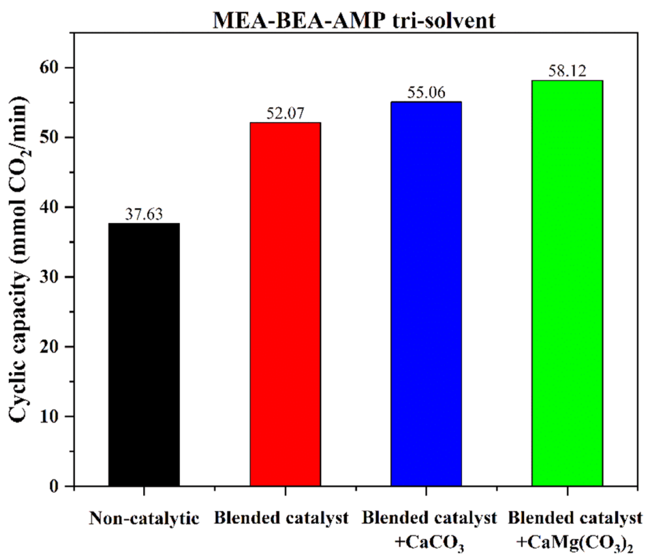

Figure 12. Effect of solid acid−base catalysts (150 g + 150 g) on cyclic capacity of trisolvent at a F_L of 70 mL/min.

reached 0.50 mol/mol, and α_{lean} returned to 0.30−0.32 mol/mol. Addition of solid acid−base catalysts enlarged the operation range of $\alpha_{lean} \sim \alpha_{rich}$ to achieve a maximum value.

Figure12 plots CC based on Figure 11 and Table 3. It followed the order: noncatalyst < H-ZSM-5/γ-Al_2O_3 (2:1) < H-ZSM-5/γ-Al_2O_3 (2:1) + $CaCO_3$ < H-ZSM-5/γ-Al_2O_3 (2:1) + $CaMg(CO_3)_2$. The order was the same as the order of $\alpha_{rich}-\alpha_{lean}$ in Table 3. Packing catalysts in absorber and desorber significantly improved the cyclic capacity. If the noncatalyst was set as bench mark (100%), the CC was 138.4% of H-ZSM-5/γ-Al_2O_3 (2:1), 146% of H-ZSM-5/γ-Al_2O_3 (2:1) + $CaCO_3$, and 154.5% of H-ZSM-5/γ-Al_2O_3 (2:1) + $CaMg(CO_3)_2$. The CC increased over 50% with the contribution of desorber catalysts to enhance CO_2 emission and absorber catalysts to accelerate CO_2 absorption simultaneously.

4.3.3. Effect of Solid Acid−Base Catalysts on Heat Duty and Temperature Profiles. The HD values of both absorber and desorber catalysts are plotted in Figure 13. The HD ranked as follows: H-ZSM-5/γ-Al_2O_3 (2:1) + $CaMg(CO_3)_2$ < H-ZSM-5/γ-Al_2O_3 (2:1) + $CaCO_3$ < H-ZSM-5/γ-Al_2O_3 (2:1) < non-catalyst; the smaller heat duty the better performance. The relative heat duty was reduced about 24.8% compared to that of

Table 3. Lean and Rich Loadings of Trisolvent MEA−BEA−AMP with Both Solid Catalysts

catalysts (150g)	rich CO_2 loading (mol CO_2/mol amine)	lean CO_2 loading (mol CO_2/mol amine)	$\alpha_{rich}-\alpha_{lean}$ (mol CO_2/mol amine)
noncatalysts	0.427	0.302	0.125
H-ZSM-5/γ-Al_2O_3 (2:1)	0.450	0.277	0.173
H-ZSM-5/γ-Al_2O_3 (2:1) + $CaCO_3$	0.501	0.318	0.183
H-ZSM-5/γ-Al_2O_3 (2:1) + $CaMg(CO_3)_2$	0.501	0.308	0.193

https://doi.org/10.1021/acsomega.3c08021
ACS Omega 2024, 9, 1838−1849

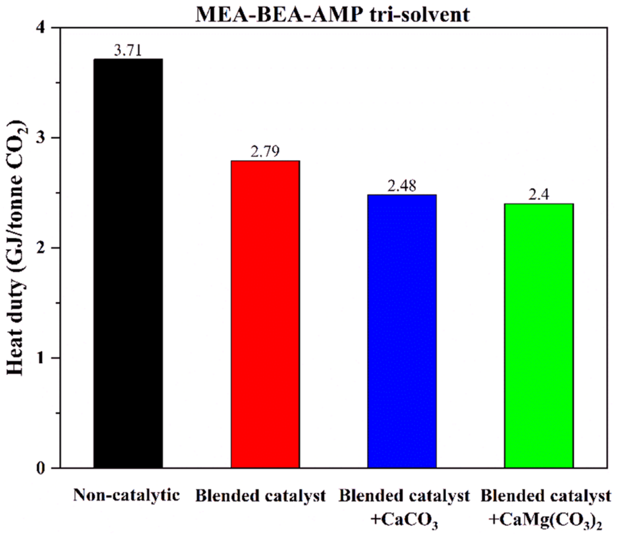

Figure 13. Effect of solid acid−base catalysts (150 g + 150 g) on heat duty of trisolvent at a F_L of 70 mL/min.

the blank with desorber catalyst H-ZSM-5/γ-Al_2O_3 (2:1). With solid base catalysts added in the absorber, the heat duty was further reduced down to 33−35%. The absorber catalyst facilitates the rate of CO_2 absorption, which made the amine approach higher loading above 0.45 mol/mol within the limited residence time. At higher α_{rich}, the CO_2−amine systems contain extra bicarbonate (HCO_3^-) than the smaller one. The energy cost of bicarbonate protonation transfer to CO_2 emission is much smaller than carbamate breakdown.[27]

The energy efficient process was MEA−BEA−AMP with H-ZSM-5/γ-Al_2O_3 (2:1) + $CaMg(CO_3)_2$, which exhibited a heat duty of 2.4 GJ/tCO_2 in Figure 13. This result is close to H-ZSM-5/γ-Al_2O_3 (2:1) + $CaCO_3$ catalysts of 2.5 GJ/tCO_2.

The temperature profiles of trisolvent with catalysts are plotted in Figure 14 for (a) absorber and (b) desorber. From Figure 14a in the absorber, the higher temperature bulge indicates faster CO_2 absorption rate. The order of temperature curve is noncatalyst < H-ZSM-5/γ-Al_2O_3 (2:1) < H-ZSM-5/γ-Al_2O_3 (2:1) + $CaCO_3$ ≈ H-ZSM-5/γ-Al_2O_3 (2:1) + $CaMg(CO_3)_2$. Such order was reasonable based on Table 3: the acid catalyst reduced α_{lean} to generate extra free amine molecules in the solvent. Extra free amine reacted with CO_2 in the absorber and released extra heat. With the aid of a solid base, the α_{rich} increased further to almost 0.50 mol/mol, representing extra CO_2 reacted with amine solvent. The temperature curves of both solid acid−base catalysts were close to each other due to their similar α_{rich} values in Table 3.

From Figure 14b in the desorber, the temperature profile follows the order of noncatalyst < H-ZSM-5/γ-Al_2O_3 (2:1) < H-ZSM-5/γ-Al_2O_3 (2:1) + $CaMg(CO_3)_2$ H-ZSM-5/γ-Al_2O_3 (2:1) + $CaCO_3$. The temperatures decreased along the desorber column because the CO_2 desorption reaction is strong endothermic. The desorption process removes heat and lowers the temperature. In the catalytic set up, the curves of both solid acid−base were higher than that of solid acid, due to its higher α_{lean} value. The α_{lean} of three sets was 0.277 mol/mol H-ZSM-5/γ-Al_2O_3 (2:1) < 0.308 mol/mol H-ZSM-5/γ-Al_2O_3 (2:1) + $CaMg(CO_3)_2$ < 0.318 mol/mol H-ZSM-5/γ-Al_2O_3 (2:1) + $CaCO_3$ in Table 3. Leaner amine solutions required extra energy to breakdown carbamate, taking away extra heat, and resulted in lower temperature.

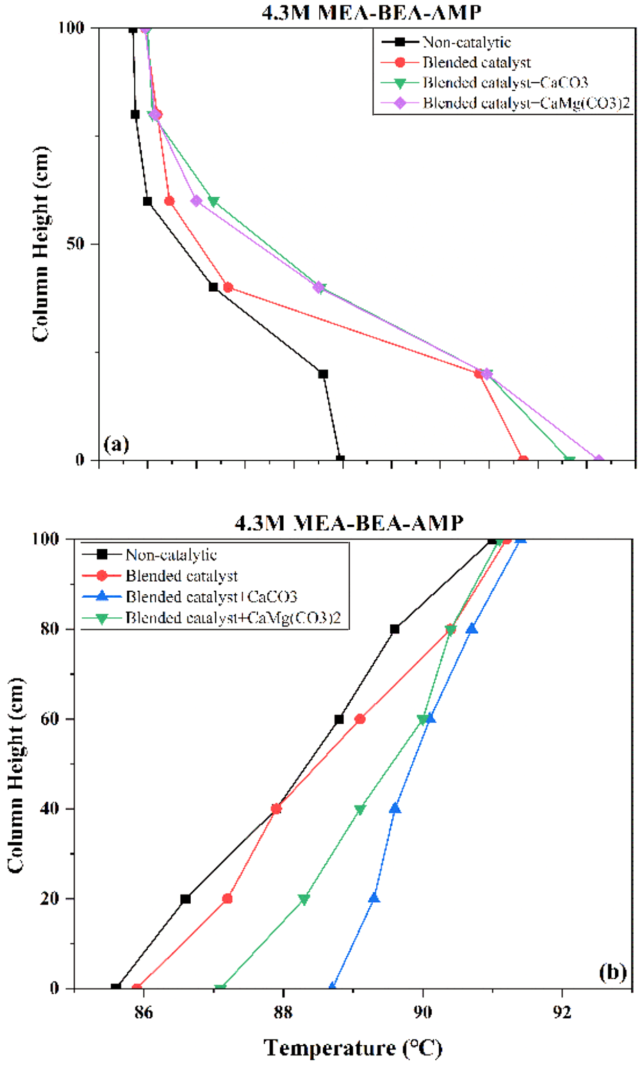

Figure 14. Effect of solid acid (a) and base (b) catalysts (150 g + 150 g) on temperature profiles of MEA−BEA−AMP at 70 mL/min.

4.4. The Cyclic Capacity and Heat Duty of Trisolvents and MEA as Benchmark. Finally, the comparison of CC and HD was conducted with trisolvent, and MEA as the benchmark with solid acid catalyst is plotted in Figure 15a,b. From Figure 15a, the CC of MEA−BEA−AMP is much better than that of MEA for all cases. The MEA systems reached optimum with 250 g of H-ZSM-5/γ-Al_2O_3, while the trisolvent reached optimum with 150 g. For HD in Figure 15b, both reached the lowest HD at 150 g of blended acid catalysts. Without catalysts, the HD reached a very high value of 12.7 GJ/tCO_2, because the hot water only could not provide adequate heat input to release CO_2 out of carbamate of MEA solvents.[23,24] Even with the aid of solid acid catalysts, the limited F_G of 3.0 L cannot remove enough CO_2, either. However, the trisolvent system absorbs a F_G of 7.0 L, and the solid catalyst can facilitate carbamate breakdown of MEA and BEA, and HCO_3^- conversion of AMP. Therefore, the HD was reduced down to 2.79 GJ/tCO_2 with massive CO_2 emission.

5. CONCLUSIONS

Effects of solid acid (H-ZSM-5/γ-Al_2O_3/HND-8) and base ($CaMg(CO_3)_2$ and $CaCO_3$) catalysts packed in the desorber and absorber of a bench-scale pilot plant of the CO_2 capture

https://doi.org/10.1021/acsomega.3c08021
ACS Omega 2024, 9, 1838−1849

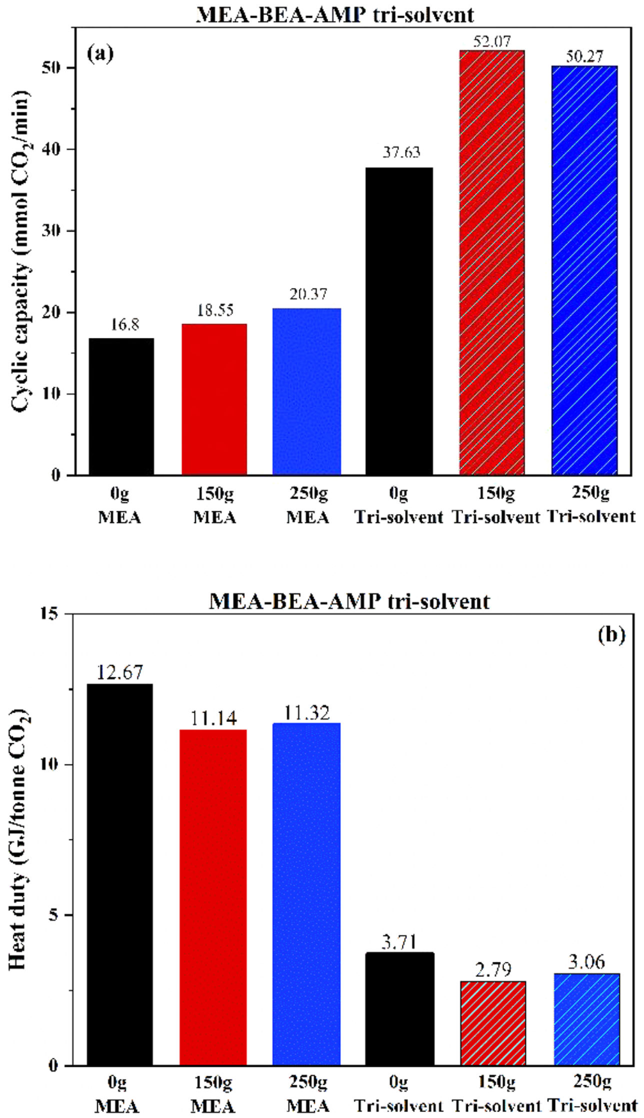

Figure 15. Effect of solid acid catalyst (H-ZSM-5/γ-Al_2O_3) on cyclic capacity (a) and heat duty (b) of MEA and MEA−BEA−AMP at a F_L of 70 mL/min.

process were evaluated on a trisolvent MEA−BEA−AMP at specific concentration in terms of cyclic capacity, absorption efficiency, and heat duty. Results showed a big improvement of the combination of trisolvent with solid acid/base catalysts compared to MEA as benchmark. Since the combination of trisolvent + catalysts was successfully tested in a bench-scale steady-state process, the performance of this absorbent + catalysts needs to be verified in a scale-up process soon, which is closer to industrial application.

For MEA solvents as benchmark, blended catalysts H-ZSM-5/γ-Al_2O_3 increased AE to 100%, increased CC at about 23%, and reduced HD about 12.0%. However, since the hot water cannot provide adequate heat input to breakdown carbamate out of MEA solvent, with small gas flow rate, the HD is very high and larger than 10 GJ/tCO_2.

For the trisolvent system with only solid acid catalyst packed, the results were clear. (1) AE increases with the increase in F_L and W_{cat}; (2) the optimized W_{cat} of trisolvent was 150 g for HD, and extra W_{cat} cannot improve AE (100%) anymore since the major contribution of solid acid was to reduce α_{lean} and release extra free amine to the absorber; (3) when AE reached 100% as optimum, any larger F_L cannot absorb extra CO_2 but it will reduce CC with smaller α_{lean} and α_{rich}, and it will increase HD with extra heat input. The solid acid catalysts were capable of desorbing CO_2 at 88−92 °C, below the boiling point of water.

With the aid of solid base catalysts in the absorber, the overall CC was better and HD was further reduced than solid acid catalysts alone in the desorber. The major contribution of absorber catalysts was to accelerate the CO_2 absorption rates for rich amine concentration within limited residence time, which increased the operation region of $\alpha_{lean} \sim \alpha_{rich}$ to enlarge CC as well as to reduce HD.

The energy efficient combination of this study was trisolvent MEA−BEA−AMP with the aid of H-ZSM-5/γ-Al_2O_3 + $CaMg(CO_3)_2$ and MEA−BEA−AMP + HND-8. Further study may test HND-8 + $CaMg(CO_3)_2$.

■ ASSOCIATED CONTENT

Supporting Information

The Supporting Information is available free of charge at https://pubs.acs.org/doi/10.1021/acsomega.3c08021.

Characterization of catalyst, reaction mechanism, CO_2 absorption rates in batch scale, and photos of the bench-scale process (PDF)

■ AUTHOR INFORMATION

Corresponding Authors

Huancong Shi − *Huzhou Institute of Zhejiang University, Huzhou, Zhejiang 313000, PR China;* orcid.org/0000-0003-4333-4118; Email: hcshi@usst.edu.cn

Jing Jin − *School of Energy and Power Engineering, University of Shanghai for Science and Technology, Shanghai 200093, PR China; Shanghai Non-carbon Energy Conversion and Utilization Institute, Shanghai 200240, China;* orcid.org/0000-0002-1681-9681; Email: alicejin001@163.com

Paitoon Tontiwachwuthikul − *Faculty of Engineering and Applied Science, University of Regina, Regina, Saskatchewan S4S 0A2, Canada;* orcid.org/0000-0003-0187-3420; Email: paitoon@uregina.ca

Mengxiang Fang − *Zhejiang University, Hangzhou, Zhejiang 310000, PR China;* orcid.org/0000-0002-3282-8756; Email: mxfang@zju.edu.cn

Authors

Nan Zhang − *School of Energy and Power Engineering, University of Shanghai for Science and Technology, Shanghai 200093, PR China*

Hanyun Wang − *State Grid New Energy Cloud Carbon Neutralization Innovation Center, Huzhou, Zhejiang 313000, PR China*

Yongcheng Feng − *Shanghai Marine Diesel Engine Research Institute, Shanghai 201108, PR China*

Complete contact information is available at: https://pubs.acs.org/10.1021/acsomega.3c08021

Notes

The authors declare no competing financial interest.

■ ACKNOWLEDGMENTS

This study was funded by Bureau of Huzhou Municipal Science and Technology (nos. 2021ZD2043 and 2021ZD2003), Bureau of Shanghai Municipal Science and Technology (no.

23010503500), and Bureau of Zhejiang Science and Technology, Software Science (no. 2023C35100).

NOMENCLATURE

C_A	amine concentration (k mol/m^3) (mol/L)
HD	heat duty (GJ/tCO_2) or (kJ/g)
P	total system pressure (kPa)
AE	absorption efficiency (%)
CC	cyclic capacity (mmol CO_2/min)
F_{G_1}	volumetric flow rate of inlet feed gas (SLPM)
F_{G_2}	volumetric flow rate of outlet off gas (SLPM)
X_{in}	CO_2 concentrations in the inlet gas
X_{out}	CO_2 concentrations in the outlet gas
F_L	flow rate of absorbent (mL/min)
R	gas constants
m_{HM}	the mass flow rate of heating medium (kg/min)
C_{PHM}	the heat capacity of heating medium (J/ (g·K)
$T_{HM,in}$, $T_{HM,out}$	temperature in and out of heating medium (K)
$\dot{m}CO_2$	mass flow rate of CO_2 product (g/min)
MW_{CO_2}	carbon dioxide captured (g/min)
W_{cat}	weight of catalysts (g)

GREEK SYMBOLS

α_{rich}	CO_2 loading of rich amine (mol of CO_2/mol amine)
α_{lean}	CO_2 loading of lean amine (mol of CO_2/mol amine)

ABBREVIATION

AMP	2-amino-2-methyl-1-propanol
BEA	Butylethanol amine
DEA	Diethanol amine
MEA	Monoethanol amine

REFERENCES

(1) Zhang, R.; Liu, R.; Barzagli, F.; Sanku, M. G.; Li, C.; Xiao, M. CO_2 absorption in blended amine solvent: Speciation, equilibrium solubility and excessive property. *Chem. Eng. J.* **2023**, *466*, 143279.

(2) Li, Y.; Chen, Z.; Yuan, B.; Xing, L.; Zhan, G.; Peng, Y.; Wang, L.; Li, J. Synergistic promotion for CO_2 absorption and solvent regeneration by fine waste red mud particles on in amine-based carbon capture: Performance and mechanism. *Sep. Purif. Technol.* **2023**, *304*, 122380.

(3) Li, Y.; Chen, Z.; Zhan, G.; Yuan, B.; Wang, L.; Li, J. Inducing efficient proton transfer through Fe/Ni@COF to promote amine-based solvent regeneration for achieving low-cost capture of CO_2 from industrial flue gas. *Sep. Purif. Technol.* **2022**, *298*, 121676.

(4) Gelowitz, D.; Supap, T.; Naami, A.; Teerawat, S.; Idem, R.; Tontiwachwuthikul, P. Part 8: Post-combustion CO_2 capture: Pilot plant operation issues. *Carbon Manage.* **2013**, *4* (2), 215−231.

(5) Idem, R.; Supap, T.; Shi, H.; Gelowitz, D.; Ball, M.; Campbell, C.; Tontiwachwuthikul, P. Practical experience in post-combustion CO_2 capture using reactive solvents in large pilot and demonstration plants. *Int. J. Greenhouse Gas Control* **2015**, *40*, 6−25.

(6) Sakwattanapong, R.; Aroonwilas, A.; Veawab, A. Behavior of Reboiler heat duty for CO_2 capture plants using regenerable single and blended alkanolamines. *Ind. Eng. Chem. Res.* **2005**, *44*, 4465−4473.

(7) Idem, R.; Wilson, M.; Tontiwachwuthikul, P.; Chakma, A.; Veawab, A.; Aroonwilas, A.; Gelowitz, D. Pilot plant studies of the CO_2 capture performance of aqueous MEA and mixed MEA/MDEA solvents at the University of Regina CO_2 capture technology development plant and the Boundary Dam CO_2 capture demonstration. *Ind. Eng. Chem. Res.* **2006**, *45* (8), 2414−2420.

(8) Liang, Z.; Rongwong, W.; Liu, H.; Fu, K.; Gao, H.; Cao, F.; Zhang, R.; Sema, T.; Henni, A.; Sumon, K.; Nath, D.; Gelowitz, D.; Srisang, W.; Saiwan, C.; Benamor, A.; Al-Marri, M.; Shi, H.; Supap, T.; Chan, C.; Zhou, Q.; Abu-Zahra, M.; Wilson, M.; Olson, W.; Idem, R.; Tontiwachwuthikul, P. Recent progress and new developments in post-combustion carbon-capture technology with amine based solvents. *Int. J. Greenhouse Gas Control* **2015**, *40*, 26−54.

(9) Tontiwachwuthikul, P.; Idem, R.; Gelowitz, D.; Liang, Z. H.; Supap, T.; Chan, C. W.; Sanpasertparnich, T.; Saiwan, C.; Smithson, H. Recent progress and new development of post-combustion carbon-capture technology using reactive solvents. *Carbon Manage.* **2011**, *2* (3), 261−263.

(10) Wang, M.; Lawal, A.; Stephenson, P.; Sidders, J.; Ramshaw, C. Post-combustion CO_2 capture with chemical absorption: A state-of-the-art review. *Chem. Eng. Res. Des.* **2011**, *89* (9), 1609−1624.

(11) Liang, Z.; Fu, K.; Idem, R.; Tontiwachwuthikul, P. Review on current advances, future challenges and consideration issues for post-combustion CO_2 capture using amine-based absorbents. *Chinese J. Chem. Eng.* **2016**, *24* (2), 278−288.

(12) Yan, J.; Zhang, Z. Carbon Capture, Utilization and Storage (CCUS). *Appl. Energy* **2019**, *235*, 1289−1299.

(13) Rochelle, G. T. Amine Scrubbing for CO_2 capture. *Science* **2009**, *325*, 1652−1654.

(14) Bernhardsen, I. M.; Knuutila, H. K. A review of potential amine solvents for CO_2 absorption process: Absorption capacity, cyclic capacity and pKa. *Int. J. Greenhouse Gas Control* **2017**, *61*, 27−48.

(15) Wu, X.; Wang, M.; Liao, P.; Shen, J.; Li, Y. Solvent-based post-combustion CO_2 capture for power plants: A critical review and perspective on dynamic modelling, system identification, process control and flexible operation. *Appl. Energy* **2020**, *257*, 113941.

(16) Alivand, M. S.; Mazaheri, O.; Wu, Y.; Stevens, G. W.; Scholes, C. A.; Mumford, K. A. Catalytic Solvent Regeneration for Energy-Efficient CO_2 Capture. *ACS Sustainable Chem. Eng.* **2020**, *8* (51), 18755−18788.

(17) de Meyer, F.; Bignaud, C. The use of catalysis for faster CO_2 absorption and energy-efficient solvent regeneration: An industry-focused critical review. *Chem. Eng. J.* **2022**, *428*, 131264.

(18) Nwaoha, C.; Odoh, K.; Ikpatt, E.; Orji, R.; Idem, R. Process simulation, parametric sensitivity analysis and ANFIS modeling of CO_2 capture from natural gas using aqueous MDEA-PZ blend solution. *J. Environ. Chem. Eng.* **2017**, *5* (6), 5588−5598.

(19) Nwaoha, C.; Smith, D. W.; Idem, R.; Tontiwachwuthikul, P. Process simulation and parametric sensitivity study of CO_2 capture from 115MW coal-fired power plant using MEA-DEA blend. *Int. J. Greenhouse Gas Control* **2018**, *76*, 1−11.

(20) Choi, J.; Cho, H.; Yun, S.; Jang, M.-G.; Oh, S.-Y.; Binns, M.; Kim, J.-K. Process design and optimization of MEA-based CO_2 capture processes for non-power industries. *Energy* **2019**, *185*, 971−980.

(21) Vega, F.; Baena-Moreno, F. M.; Gallego Fernández, L. M.; Portillo, E.; Navarrete, B.; Zhang, Z. Current status of CO_2 chemical absorption research applied to CCS: Towards full deployment at industrial scale. *Appl. Energy* **2020**, *260*, 114313.

(22) ElMoudir, W.; Supap, T.; Saiwan, C.; Idem, R.; Tontiwachwuthikul, P. Part 6: Solvent recycling and reclaiming issues. *Carbon Manage.* **2012**, *3* (5), 485−509.

(23) Srisang, W.; Pouryousefi, F.; Osei, P. A.; Decardi-Nelson, B.; Akachuku, A.; Tontiwachwuthikul, P.; Idem, R. Evaluation of the heat duty of catalyst-aided amine-based post combustion CO_2 capture. *Chem. Eng. Sci.* **2017**, *170*, 48−57.

(24) Srisang, W.; Pouryousefi, F.; Osei, P. A.; Decardi-Nelson, B.; Akachuku, A.; Tontiwachwuthikul, P.; Idem, R. CO_2 capture efficiency and heat duty of solid acid catalyst-aided CO_2 desorption using blends of primary-tertiary amines. *Int. J. Greenhouse Gas Control* **2018**, *69*, 52−59.

(25) Natewong, P.; Prasongthum, N.; Reubroycharoen, P.; Idem, R. Evaluating the CO_2 Capture Performance Using a BEA-AMP Biblend Amine Solvent with Novel High-Performing Absorber and Desorber Catalysts in a Bench-Scale CO_2 Capture Pilot Plant. *Energ Fuel* **2019**, *33* (4), 3390−3402.

(26) Afari, D. B.; Coker, J.; Narku-Tetteh, J.; Idem, R. Comparative Kinetic Studies of Solid Absorber Catalyst (K/MgO) and Solid Desorber Catalyst (HZSM-5)-Aided CO_2 Absorption and Desorption

from Aqueous Solutions of MEA and Blended Solutions of BEA-AMP and MEA-MDEA. *Ind. Eng. Chem. Res.* **2018**, *57* (46), 15824−15839.

(27) Narku-Tetteh, J.; Afari, D. B.; Coker, J.; Idem, R. Evaluation of the Roles of Absorber and Desorber Catalysts in the Heat Duty and Heat of CO_2 Desorption from BEA-AMP and MEA-MDEA Solvent Blends in a Bench-Scale CO_2 Capture Pilot Plant. *Energ Fuel* **2018**, *32* (9), 9711−9726.

(28) Akachuku, A.; Osei, P. A.; Decardi-Nelson, B.; Srisang, W.; Pouryousefi, F.; Ibrahim, H.; Idem, R. Experimental and kinetic study of the catalytic desorption of CO_2 from CO_2-loaded monoethanolamine (MEA) and blended monoethanolamine − Methyl-diethanolamine (MEA-MDEA) solutions. *Energy* **2019**, *179*, 475−489.

(29) Prasongthum, N.; Natewong, P.; Reubroycharoen, P.; Idem, R. Solvent Regeneration of a CO_2-Loaded BEA-AMP Bi-Blend Amine Solvent with the Aid of a Solid Bronsted $Ce(SO_4)_2/ZrO_2$ Superacid Catalyst. *Energ Fuel* **2019**, *33* (2), 1334−1343.

(30) Sema, T.; Naami, A.; Liang, Z.; Shi, H.; Rayer, A. V.; Sumon, K. Z.; Wattanaphan, P.; Henni, A.; Idem, R.; Saiwan, C.; Tontiwachwuthikul, P. Part 5b: Solvent chemistry: Reaction kinetics of CO_2 absorption into reactive amine solutions. *Carbon Manage.* **2012**, 3 (2), 201−220.

(31) Shi, H.; Zhou, Y.; Zuo, Y.; Cui, L.; Idem, R.; Tontiwachwuthikul, P. Heterogeneous catalysis of CO_2-diethanolamine absorption with $MgCO_3$ and $CaCO_3$ and comparing to non-catalytic CO_2-monoethanolamine interactions. *React. Kinet., Mech. Catal.* **2017**, *122* (1), 539−555.

(32) Shi, H.; Huang, M.; Huang, Y.; Cui, M.; Idem, R. Catalytic CO_2-MEA absorptions with the aid of $CaCO_3$, $MgCO_3$, and $BaCO_3$ in the batch and semi-batch processes. *Chem. Eng. Commun.* **2020**, *207* (4), 506−522.

(33) Shi, H.; Huang, M.; Huang, Y.; Cui, M.; Rapheal, I. CO_2 absorption effieicency of various MEA-DEA blend with aid of $CaCO_3$ and $MgCO_3$ in a batch and semi-batch processes. *Sep. Purif. Technol.* **2019**, *220*, 102−113.

(34) Shi, H.; Huang, M.; Wu, Q.; Zheng, L.; Cui, L.; Zhang, S.; Tontiwachwuthikul, P. Study of Catalytic CO_2 Absorption and Desorption with Tertiary Amine DEEA and 1DMA-2P with the Aid of Solid Acid and Solid Alkaline Chemicals. *Molecules* **2019**, *24*, 6.

(35) Shi, H.; Huang, M.; Huang, Y.; Cui, M.; Idem, R. CO_2 absorption efficiency of various MEA-DEA blend with aid of $CaCO_3$ and $MgCO_3$ in a batch and semi-batch processes. *Sep. Purif. Technol.* **2019**, *220*, 102−113.

(36) Shi, H.; Huang, M.; Huang, Y.; Cui, L.; Zheng, L.; Jiang, L.; Ibrahim, H.; Tontiwachwuthikul, P. Eley-Rideal model of heterogeneous catalytic carbamate formation based on CO_2-MEA absorptions with $CaCO_3$, $MgCO_3$ and $BaCO_3$. *R. Soc. Open Sci.* **2019**, *6*, 190311−190332.

(37) Narku-Tetteh, J.; Muchan, P.; Saiwan, C.; Supap, T.; Idem, R. Selection of components for formulation of amine blends for post combustion CO_2 capture based on the side chain structure of primary, secondary and tertiary amines. *Chem. Eng. Sci.* **2017**, *170*, 542−560.

(38) Shi, H.; Cui, M.; Fu, J.; Dai, W.; Huang, M.; Han, J.; Quan, L.; Tontiwachwuthikul, P.; Liang, Z. Application of "coordinative effect" into tri-solvent MEA+BEA+AMP blends at concentrations of 0.1 + 2 + 2 ∼ 0.5 + 2 + 2 mol/L with absorption, desorption and mass transfer analyses. *Int. J. Greenhouse Gas Control* **2021**, *107*, 103267.

(39) Shi, H.; Yang, X.; Feng, H.; Fu, J.; Zou, T.; Yao, J.; Wang, Z.; Jiang, L.; Tontiwachwuthikul, P. Evaluating Energy-Efficient Solutions of CO_2 Capture within Tri-solvent MEA+BEA+AMP within 0.1 + 2+2−0.5 + 2+2 mol/L Combining Heterogeneous Acid−Base Catalysts. *Ind. Eng. Chem. Res.* **2021**, *60* (19), 7352−7366.

(40) Shi, H.; Cheng, X.; Peng, J.; Feng, H.; Tontiwachwuthikul, P.; Hu, J. The CO_2 absorption and desorption analysis of tri-solvent MEA + EAE + AMP compared with MEA + BEA + AMP along with "coordination effects" evaluation. *Environ. Sci. Pollut. Res.* **2022**, *29*, 40686−40700.

(41) Xiao, S.; Liu, H.; Gao, H.; Xiao, M.; Luo, X.; Idem, R.; Tontiwachwuthikul, P.; Liang, Z. Kinetics and mechanism study of homogeneous reaction of CO_2 and blends of diethanolamine and monoethanolamine using the stopped-flow technique. *Chem. Eng. J.* **2017**, *316*, 592−600.

(42) Liu, H.; Li, M.; Luo, X.; Liang, Z.; Idem, R.; Tontiwachwuthikul, P. Investigation mechanism of DEA as an activator on aqueous MEA solution for postcombustion CO_2 capture. *AIChE J* **2018**, *64* (7), 2515−2525.

(43) Shi, H.; Fu, J.; Wu, Q.; Huang, M.; Jiang, L.; Cui, M.; Idem, R.; Tontiwachwuthikul, P. Studies of the coordination effect of DEA-MEA blended amines (within 1 + 4 to 2 + 3 M) under heterogeneous catalysis by means of absorption and desorption parameters. *Sep. Purif. Technol.* **2020**, *236*, 116179.

(44) Xie, H.-B.; Zhou, Y.; Zhang, Y.; Johnson, J. K. Reaction mechanism of MEA with CO_2 in aqueous solution from molecular modeling. *J. Phys. Chem. A* **2010**, *114*, 11844−11852.

(45) Muchan, P.; Saiwan, C.; Narku-Tetteh, J.; Idem, R.; Supap, T.; Tontiwachwuthikul, P. Screening tests of aqueous alkanolamine solutions based on primary, secondary, and tertiary structure for blended aqueous amine solution selection in post combustion CO_2 capture. *Chem. Eng. Sci.* **2017**, *170*, 574−582.

(46) Muchan, P.; Narku-Tetteh, J.; Saiwan, C.; Idem, R.; Supap, T. Effect of number of amine groups in aqueous polyamine solution on carbon dioxide (CO_2) capture activities. *Sep. Purif. Technol.* **2017**, *184*, 128−134.

(47) Liang, Z.; Idem, R.; Tontiwachwuthikul, P.; Yu, F.; Liu, H.; Rongwong, W. Experimental study on the solvent regeneration of a CO_2-loaded MEA solution using single and hybrid solid acid catalysts. *AIChE J.* **2016**, *62* (3), 753−765.

(48) Liu, H.; Zhang, X.; Gao, H.; Liang, Z.; Idem, R.; Tontiwachwuthikul, P. Investigation of CO_2 Regeneration in Single and Blended Amine Solvents with and without Catalyst. *Ind. Eng. Chem. Res.* **2017**, *56* (27), 7656−7664.

(49) Shi, H.; Zheng, L.; Huang, M.; Zuo, Y.; Kang, S.; Huang, Y.; Idem, R.; Tontiwachwuthikul, P. Catalytic-CO_2-Desorption Studies of DEA and DEA-MEA Blended Solutions with the Aid of Lewis and Bronsted Acids. *Ind. Eng. Chem. Res.* **2018**, *57* (34), 11505−11516.

(50) Horwitz, W.. *Association of Official Analytical Chemists (AOAC) Methods*; George Banta Co.: Menasha, WI, USA, 1975.

(51) Shi, H.; Naami, A.; Idem, R.; Tontiwachwuthikul, P. Catalytic and non catalytic solvent regeneration during absorption-based CO_2 capture with single and blended reactive amine solvents. *Int. J. Greenhouse Gas Control* **2014**, *26*, 39−50.

(52) Fu, K.; Sema, T.; Liang, Z.; Liu, H.; Na, Y.; Shi, H.; Idem, R.; Tontiwachwuthikul, P. Investigation of Mass-Transfer Performance for CO_2 Absorption into Diethylenetriamine (DETA) in a Randomly Packed Column. *Ind. Eng. Chem. Res.* **2012**, *51* (37), 12058−12064.

(53) Naami, A.; Edali, M.; Sema, T.; Idem, R.; Tontiwachwuthikul, P. Mass Transfer Performance of CO_2 Absorption into Aqueous Solutions of 4-Diethylamino-2-butanol, Monoethanolamine, and N-Methyldiethanolamine. *Ind. Eng. Chem. Res.* **2012**, *51* (18), 6470−6479.

(54) Zhang, X.; Hong, J.; Liu, H.; Luo, X.; Olson, W.; Tontiwachwuthikul, P.; Liang, Z. $SO_4^{2}-/ZrO_2$ supported on γ-Al_2O_3 as a catalyst for CO_2 desorption from CO_2-loaded monoethanolamine solutions. *AIChE J.* **2018**, *64* (11), 3988−4001.

(55) Zhang, X.; Liu, H.; Liang, Z.; Idem, R.; Tontiwachwuthikul, P.; Jaber Al-Marri, M.; Benamor, A. Reducing energy consumption of CO_2 desorption in CO_2-loaded aqueous amine solution using Al_2O_3/HZSM-5 bifunctional catalysts. *Appl. Energy* **2018**, *229*, 562−576.

(56) Wang, L.; Yao, M.; Hu, X.; Hu, G.; Lu, J.; Luo, M.; Fan, M. Amine-modified ordered mesoporous silica: The effect of pore size on CO_2 capture performance. *Appl. Surf. Sci.* **2015**, *324*, 286−292.

(57) Ko, Y. G.; Shin, S. S.; Choi, U. S. Primary, secondary, and tertiary amines for CO_2 capture: Designing for mesoporous CO_2 adsorbents. *J. Colloid Interface Sci.* **2011**, *361* (2), 594−602.

https://doi.org/10.1021/acsomega.3c08021
ACS Omega 2024, 9, 1838−1849